Orthotropic fluid diffusion in composite marine structures. Experimental procedure, analytical and numerical modelling of plates, rods and pipes

Abedin I. Gagani, Andrey E. Krauklis, Andreas T. Echtermeyer

Department of Mechanical and Industrial Engineering, Norwegian University of Science and Technology (NTNU), Trondheim, Norway

Corresponding author: abedin.gagani@ntnu.no +47 7359 3885

Abstract

Finite elements simulations of fluid diffusion for composite structures are becoming more common in marine and offshore applications. Input parameters for such simulations are the orthotropic diffusion constants for the materials. Diffusivity in fiber direction is faster than diffusivity in transverse direction; it is therefore important to determine all these constants to predict long-term fluid diffusion in composite structures. Current standards for the determination of the diffusion constants prescribe a sample geometry that enforces 1-D diffusion, but thin samples are not easy to fabricate, especially from thick laminates. Edges with metallic coatings are also prescribed, which can influence the calculation of the moisture saturation content and may detach during the experiments. Furthermore, axial symmetrical structures are often used offshore, requiring 3-D diffusion analysis in cylindrical coordinates. The aim of this paper is to provide a 3-D theory and methods for obtaining diffusion constants for plates, rods and pipes.

Keywords: Polymer-matrix composites (PMCs); Environmental degradation; Analytical modelling; Moisture; Resin transfer moulding (RTM).

List of symbols

α	Solution of the zero-th order Bessel function
c	Moisture concentration
c_0	Moisture initial concentration
D_{11}, D_{22}, D_{33}	Orthotropic diffusion constants in cartesian coordinates
$D_{\parallel}$, $D_{\perp}$	Parallel to fiber and transverse to fibers diffusion constants
D_R, D_Z	Composite orthotropic diffusion constants in cylindrical coordinates
h, l, w	Laminate thickness, length and width
J_0, Y_0	Bessel functions of first and second order
L, R, R_e, R_i	Length of rod and pipe, rod radius, pipe external and internal radius
M(t), M_{eq}	Moisture content and moisture saturation content
r, z, ϕ	Cylindrical coordinate system
t	Time
x, y, z	Cartesian coordinate system

1. Introduction

The prediction of long-term performance of composite structures exposed to humid environments requires knowledge of the fluid concentration profiles inside the component. Such concentration profiles can be obtained by means of finite element (FE) analysis, which require knowledge of the orthotropic diffusion constants and moisture saturation content of the material. Obtaining the fluid diffusion orthotropic constants is often a bottleneck. Composite materials have orthotropic diffusion constants, as shown by many studies [1-8]. Typically, diffusion in the fiber direction can be 3-15 times higher than in transverse direction, and this can accelerate fluid saturation greatly [4-6, 9].

The gravimetric testing method proposed in ASTM Standard D5229 [10] is very useful for obtaining the transverse diffusivity of a composite, but obtaining the other two orthotropic

diffusion constants using this method remains challenging. Furthermore, the applicability of the standard is limited to thin plates. Rods and pipes are not dealt with using this method.

Using ASTM Standard D5229 it is possible to obtain the diffusivity of a composite material in an arbitrary direction, by preparing a thin sample (the thickness to width ratio suggested is 1/100) and coating with a stainless-steel foil the edges of the sample.

Preparing such thin samples can be non-trivial, especially for the diffusion in the fiber direction, because samples are often obtained from laminates having reduces initial thickness. For example, from a 30 mm thick laminate, in order to study diffusion in the fiber direction it is necessary to slice the laminate orthogonally to the fiber, to a final thickness of 0.3 mm. Such a sample would weigh only half gram and measuring a 0.1% mass increase in such case would require a very sensitive, hence expensive, scale.

Another complication involved with this method is the use of stainless-steel foil for covering the edges. Firstly, in order to bond the foil to the edges an adhesive is necessary, and this adhesive would absorb water in most cases, influencing the weight gain measurements. Furthermore, the bonding between a metallic foil and a thin composite edge surface is not very strong, and the stainless-steel foil could peel off or fall off from the sample, severely disturbing the data.

In order to overcome these issues, some authors have proposed measuring diffusivity of composites without coating the samples edges but taking into account the 3-dimensional fluid diffusion equations [6, 8, 11-13].

Composite structures used in offshore industry have often non-flat shapes, like pultruded composite rods [14] and filament wound pipes [15, 16]. For such structures the test method suggested in the standard [10] cannot be used to obtain radial and axial diffusion constants. In this work exact and approximate analytical solutions are introduced for orthotropic diffusion

in pipes. Together with a novel test method, based on testing long radial diffusion dominated and short axial diffusion dominated samples, it is possible to identify axial and radial diffusion constants. The results are compared to known solutions for plates and rods made from the same material and also tested in this work, to assess the accuracy of the method. These geometries: plates, rods and pipes, are representative of structural applications of composites offshore:

- Repair patches [17, 18],
- Tension-leg-platform (TLP) tethers [14],
- Offshore risers [15, 16].

In this article sample configurations and equations for obtaining orthotropic diffusion constants are proposed. The approach is based on testing sample having geometries that promote either mono-dimensional or multi-dimensional diffusion, in Cartesian or cylindrical coordinates. A regression of the experimental results with the analytical or FE models reported here enables identification of the orthotropic diffusion constants. Experiments were carried out to demonstrate how the procedures work and to show typical analysis of the results.

2. Materials and methods

The glass fibers used were HiPer-Tex^{TM} unidirectional fabric from 3B. The epoxy was supplied by Hexion and consisted in RIMR135^{TM} resin and RIMH137^{TM} hardener with a mass mixing ratio of 100:30. A thick laminate was prepared by vacuum assisted resin infusion of 32 plies. Curing was performed at room temperature for 24 hours and post-curing was performed at 80°C for 16 hours, according to the manufacturer's recommendations [19]. Three bars were cut from the laminate along the fiber direction. From one of the bars four

plates have been cut orthogonally to the fiber direction and four plates have been cut along the fiber direction, using a water-cooled diamond saw. The samples were later milled and ground to the dimensions: 24 x 24 x 1.5 mm.

Another bar obtained from the same laminate was used in order to prepare 6 mm diameter rods, using a turning machine. Four “long” rods and four “short” rods were manufactured, having length 30 and 6 mm respectively.

From another bar, obtained from the same laminate, pipes having internal diameter 20 mm and external diameter 24 mm were manufactured, using a turning machine. Four “long” pipes and four “short” pipes were turned, having length 24 and 2 mm respectively.

Composite pipes and rods are often obtained using different manufacturing processes, typically filament winding and pultrusion. In this work it was decided to obtain all the samples from the same laminate, in order to consistently compare the diffusion constants obtained from the different samples configurations. The fiber volume fraction for all samples was measured according to the burn off test [20] resulting in 54.4 %. Samples dimensions are summarized in **Table 1** and sample pictures are shown in **Fig.1**.

Table 1. Sample geometry for each configuration

Geometry	Samples for radial/transverse diffusivity	Samples for axial diffusivity
Rods	R= 3, L= 30	R= 3, L= 6
Pipes	R_e= 12, R_i= 10, L= 24	R_e= 12, R_i= 10, L= 2
Plates	l= 24, w= 24, h= 1.5	

L: rod/pipe/plate length, R: rod radius, R_e: pipe external radius, R_i: pipe internal radius, w: plate width, h: plate thickness

Fig. 1. Sample configurations tested

Before conditioning the samples were dried in oven for 72 hr at 40°C, in order to remove moisture diffusing in the material during the manufacturing process.

The fluid diffusion test was performed according to the standard [10], in distilled water at 60°C ± 1 ˚C. This temperature was chosen in order to opportunely accelerate fluid diffusion while still remaining below the glass temperature of the material: 87.1°C, measured using dynamic mechanical analysis (DMA). The samples were removed regularly from the water bath four at a time, their surface dried with a cloth and their mass recorded immediately using a Mettler Toledo AG 204 DeltaRange scale, having sensitivity 0.1 mg.

Fig. 2. Sample configurations for plates, rods and pipes. It can be noticed that for rods and pipes the axial direction coincides with the laminate fiber direction

3. Analytical model

The analytical model reported here is based on the following assumptions:

- fickian diffusion;
- transversely isotropic material.

It is important to remark that the solutions reported here are valid for arbitrary dimension. It is not necessary to assume infinitely thin plates or infinitely long rods or pipes.

3.1 Composite plates

Fick's 2nd law for orthotropic materials in cartesian coordinates is:

$$\frac{\partial c}{\partial t} = \nabla \cdot (\mathrm{D}\,\nabla c) = D_{11}\frac{\partial^2 c}{\partial x^2} + D_{22}\frac{\partial^2 c}{\partial y^2} + D_{33}\frac{\partial^2 c}{\partial z^2} \quad (1)$$

where c(*x*,*t*) is fluid concentration, *t* is time, *x*,*y*,*z* are the coordinates in cartesian space, D is the positive definite symmetric matrix of diffusion coefficients D_{ij}, and D_{11}, D_{22} and D_{33} are the diffusion constants in directions 1, 2 and 3 respectively.

It is assumed here that direction 1 is the fiber axial direction, direction 2 is transverse in plane direction and direction 3 is transverse out of plane direction, as shown in **Fig. 2**.

For a plate having length l, width w and thickness h, the boundary conditions representing immersion in a fluid of an initially dry sample are:

for t = 0

$$c\,(x, y, z) = 0 \quad (2)$$

for t > 0

$$c\left(+\frac{l}{2}\right) = c\left(-\frac{l}{2}\right) = c_0 \quad (3)$$

$$c\left(+\frac{w}{2}\right) = c\left(-\frac{w}{2}\right) = c_0 \quad (4)$$

$$c\left(+\frac{h}{2}\right) = c\left(-\frac{h}{2}\right) = c_0 \quad (5)$$

the solution of this problem is provided by Crank [21]. For the transverse plate configuration, **Fig. 3 (a)**, the solution is:

$$M(t) = M_{eq}\left[1 - \left(\frac{8}{\pi^2}\right)^3 \sum_{i=1}^{\infty}\sum_{j=1}^{\infty}\sum_{k=1}^{\infty} \frac{1}{(2i-1)^2} e^{-(2i-1)^2\left(\frac{\pi}{l}\right)^2 D_{11}t} \cdot \frac{1}{(2j-1)^2} e^{-(2j-1)^2\left(\frac{\pi}{w}\right)^2 D_{22}t} \cdot \frac{1}{(2k-1)^2} e^{-(2k-1)^2\left(\frac{\pi}{h}\right)^2 D_{33}t}\right] \quad (6)$$

Fig. 3. (a) Transverse plate geometry, **(b)** Axial plate geometry

For a transversely isotropic material, having $D_{22} = D_{33} = D_{\perp}$ and $D_{11} = D_{\parallel}$, Eq. (6) becomes:

$$M(t) = M_{eq}\left[1 - \left(\frac{8}{\pi^2}\right)^3 \sum_{i=1}^{\infty}\sum_{j=1}^{\infty}\sum_{k=1}^{\infty} \frac{1}{(2i-1)^2} e^{-(2i-1)^2\left(\frac{\pi}{l}\right)^2 D_{\parallel} t} \cdot \frac{1}{(2j-1)^2} e^{-(2j-1)^2\left(\frac{\pi}{w}\right)^2 D_{\perp} t} \cdot \frac{1}{(2k-1)^2} e^{-(2k-1)^2\left(\frac{\pi}{h}\right)^2 D_{\perp} t}\right] \quad (7)$$

For the axial plate configuration, **Fig. 3 (b)**, under the hypothesis of orthotropic material:

$$M(t) = M_{eq}\left[1 - \left(\frac{8}{\pi^2}\right)^3 \sum_{i=1}^{\infty}\sum_{j=1}^{\infty}\sum_{k=1}^{\infty} \frac{1}{(2i-1)^2} e^{-(2i-1)^2\left(\frac{\pi}{l}\right)^2 D_{33} t} \cdot \frac{1}{(2j-1)^2} e^{-(2j-1)^2\left(\frac{\pi}{w}\right)^2 D_{22} t} \cdot \frac{1}{(2k-1)^2} e^{-(2k-1)^2\left(\frac{\pi}{h}\right)^2 D_{11} t}\right] \quad (8)$$

For a transversely isotropic material, having $D_{22} = D_{33} = D_{\perp}$ and $D_{11} = D_{\parallel}$, Eq. (8) becomes:

$$M(t) = M_{eq}\left[1 - \left(\frac{8}{\pi^2}\right)^3 \sum_{i=1}^{\infty}\sum_{j=1}^{\infty}\sum_{k=1}^{\infty} \frac{1}{(2i-1)^2} e^{-(2i-1)^2\left(\frac{\pi}{l}\right)^2 D_{\perp} t} \cdot \frac{1}{(2j-1)^2} e^{-(2j-1)^2\left(\frac{\pi}{w}\right)^2 D_{\perp} t} \cdot \frac{1}{(2k-1)^2} e^{-(2k-1)^2\left(\frac{\pi}{h}\right)^2 D_{\parallel} t}\right] \quad (9)$$

3.2 Composite rods

Fick's 2nd law for orthotropic materials in radial coordinates is [21, 22]:

$$\frac{\partial c}{\partial t} = D_Z \frac{\partial^2 c}{\partial z^2} + D_R \frac{1}{r}\frac{\partial}{\partial r}\left(r \frac{\partial c}{\partial r}\right) \quad (10)$$

where $c(x,t)$ is fluid concentration, t is time, r the radial coordinate, z the axial coordinate, D_R the radial diffusion constant and D_Z the axial diffusion constant. Eq. (10) assumes axial symmetry and finite length.

For a cylinder having radius R and length 2L, as in **Fig.4**, the boundary conditions representing immersion in a fluid of an initially dry sample are:

for t = 0

$$c(r,z) = 0 \tag{11}$$

for t > 0

$$c(R,z) = c_0 \tag{12}$$

$$c(r,\pm L) = c_0 \tag{13}$$

Fig. 4. Coordinate system and dimensions for a composite rod

the solution of this problem is reported in [9, 22] and is:

$$M(t) = M_{eq}\left\{1 - \frac{32}{\pi}\sum_{m=1}^{\infty}\sum_{n=0}^{\infty}\frac{1}{(\alpha_m)^2}\exp\left(\frac{-\alpha_m^2 D_R\, t}{R^2}\right)\cdot\frac{1}{(2n+1)^2}\exp\left[-\frac{(2n+1)^2\pi^2}{4L^2}\, D_Z t\right]\right\} \tag{14}$$

where L is the half length of the cylinder, D_R the radial diffusion constant, D_Z the axial diffusion constant and α_m the roots of Bessel function of order zero: $J_0(\alpha_m) = 0$.

3.3 Composite pipes

For an orthotropic pipe, the radial and axial diffusion constants can be obtained from the weight gain measurements of long and short pipes, as shown in **Figs. 1-2**.

Fluid diffusion in an orthotropic pipe is described by the same equation introduced for fluid diffusion in a rod, Eq. (10):

$$\frac{\partial c}{\partial t} = D_Z\frac{\partial^2 c}{\partial z^2} + D_R\frac{1}{r}\frac{\partial}{\partial r}\left(r\frac{\partial c}{\partial r}\right) \tag{15}$$

where c(*x*,*t*) is fluid concentration, *t* is time, *r* the radial coordinate, *z* the axial coordinate, D_R the radial diffusion constant and D_Z the axial diffusion constant.

For a hollow cylinder, having the geometry shown in **Fig. 5**, the boundary conditions simulating immersion of an initially dry sample are:

for t = 0

$$c\,(r,z) = 0 \tag{16}$$

for t > 0

$$c\,(R_i,z) = c_0 \tag{17}$$

$$c\,(R_e,z) = c_0 \tag{18}$$

$$c\,(r,\pm L) = c_0 \tag{19}$$

Fig. 5. Coordinate system and dimensions for a composite pipe

The solution of this problem can be obtained with simple derivation from [9, 21]:

$$M(t) = M_\infty \left[1 - \frac{32}{\pi^2\left(R_e{}^2 - R_i{}^2\right)} \sum_{n=1}^{\infty} \sum_{m=0}^{\infty} \frac{J_0(R_i\alpha_n) - J_0(R_e\alpha_n)}{\alpha_n{}^2 [J_0(R_i\alpha_n) + J_0(R_e\alpha_n)]} exp(-D_R \alpha_n{}^2\, t) \cdot \right.$$

$$\left. \frac{1}{(2n+1)^2} exp\left(-\frac{(2m+1)^2\pi^2}{4L^2} D_Z t\right)\right] \tag{20}$$

where α_n are roots of the equation:

$$J_0(R_i\,\alpha_n)\,Y_0(R_e\,\alpha_n) - J_0(R_e\,\alpha_n)\,Y_0(R_i\,\alpha_n) = 0 \tag{21}$$

where J_0 and Y_0 are the Bessel functions of first and second kind.

The solution proposed in Eq. (20) is valid for arbitrary thick pipes. For thick-walled pipes, the samples can take very long time to saturate. In this case an alternative possibility is slicing plates from the pipes, as shown in **Fig. 6**. From the plates the directional diffusivities can be obtained using the plate diffusion solutions reported in the previous paragraph, using Eq. (7) for radial diffusivity and Eq. (9) for axial diffusivity.

Fig. 6. Schematic drawing on obtaining axial and radial diffusion plates from a thick-walled pipe

3.4 Approximated 2-D plate solution for orthotropic pipes

An axial symmetric thin-walled pipe can be modelled as an equivalent infinitely wide plate, having the same length of the pipe, 2 L, and thickness equal to the pipe wall thickness, $R_e - R_i$, as shown in **Fig. 7**.

Fig. 7. Approximation of thin-walled pipe to equivalent infinitely wide plate

In this case, the solution reported in Eq. (20) can be replaced by the two-dimensional solution of fluid diffusion in an infinitely wide rectangular plate having the same length as the pipe and thickness equal to the pipe wall thickness:

$$M(t) = M_{eq}\left[1 - \left(\frac{8}{\pi^2}\right)^2 \sum_{i=1}^{\infty}\sum_{j=1}^{\infty} \frac{1}{(2i-1)^2} e^{-(2i-1)^2\left[\frac{\pi}{(R_e-R_i)}\right]^2 D_R t} \cdot \frac{1}{(2j-1)^2} e^{-(2j-1)^2\left(\frac{\pi}{2L}\right)^2 D_Z t}\right] \quad (22)$$

It is interesting to obtain an equivalent plate solution, for two reasons. The first one is that plate solutions are easier to implement as they don't invoke the zeros of the Bessel function,

while the second one is that several models have been published dealing with the influence of matrix transverse cracks on diffusivity in composite plates [23, 24]. These models can be easily implemented for composite pipes having transverse matrix cracks, using the approximated plate solution as a starting point.

The accuracy of the approximated solution is shown, as a function of the wall thickness of the pipe in the **Appendix**. For the material studied here, the approximated solution showed has a good accuracy even for thick-walled pipes.

4. Numerical model

The previous paragraph has shown the exact analytical solutions for fluid diffusion in plates, rods and pipes, and the approximated solution for pipes. The fluid diffusion of these geometries can be analysed also by means of finite element (FE), as shown in this paragraph. For complex geometries analytical solutions become hard to integrate and FE modelling remains a strong alternative. For this reason, the numerical modelling methodology is shown here.

The finite element analysis was performed in Abaqus^{TM}, using a diffusion step analysis. A 1/8 symmetric 3D model was used for the plates and axial symmetric 2D model for the rods and pipes, **Fig.8**.

Fig. 8. FE models used for the plate, rod and pipe. The surfaces exposed to fluid diffusion are indicated by the arrows

The elements used were DC3D8 for the plates (8-node linear heat transfer brick) and DCAX4 for the rods and pipes (4-node linear axisymmetric heat transfer quadrilateral). Element size for the plates was 0.25 mm and 0.1 in the thickness direction. Element size for the rods and pipes was 0.1 mm overall. These element sizes were chosen after a mesh sensitivity analysis.

5. Results

The weight gain curves are shown in **Fig. 9 (a-c)** for composite plates, rods and pipes.

Fig. 9. Experimental weight gain curves of: (a) plates, (b) rods and (c) pipes.

Moisture saturation content for each configuration was obtained as an average of four parallel measurements. Mean values and standard deviations are reported in **Fig. 10**.

Fig. 10. Moisture saturation content for each configuration

The average value obtained was 0.775%, with a minimum of 0.72% and a maximum of 0.86% (16% deviation between maximum and minimum, 2% standard deviation). The moisture saturation content is a material property and should ideally be the same for all configurations. The reason for this difference is attributed to the different manufacturing processes, which lead to different surface roughness and porosity.

A regression analysis was performed on all sample geometries (plates, rods and pipes) based on the analytical solutions, Eqs. (9,14,20), in order to obtain the diffusivities for each configuration. The diffusivities were obtained by performing nonlinear Generalized Reduced Gradient (GRG) algorithm, while minimizing the residual sum of squares. The algorithm was

used iteratively within each geometry (plates, rods and pipes) in order to obtain D_R (or $D_\perp$) and D_Z (or $D_\parallel$). Diffusivities obtained via regression analysis are shown in **Fig. 11**.

Fig. 11. Diffusivities for each geometry (plates, rods, pipes)

Diffusivities obtained for all three geometries are in good agreement with each other. Results indicate that diffusivities obtained for plate geometry provide less scatter than rods and even more so than pipes.

The diffusion constants obtained from the regression analysis have been then used as input material properties for the FE analysis. The weight gain curves obtained by theoretical and FE analysis were plotted along with experimental results in **Fig. 9** (a-c).

The values of diffusivities obtained from the regression analysis are reported in **Table 2**.

Table 2. Diffusion constants obtained from the regression analysis

Configuration	Transverse/Radial diffusivity (mm^2/h)	Axial diffusivity (mm^2/h)
Plates	0.0043 ± 0.0004	0.0105 ± 0.0004
Rods	0.0041 ± 0.0005	0.0099 ± 0.0012
Pipes	0.0038 ± 0.0008	0.0133 ± 0.0030
AVERAGE	0.0041	0.0113

From what has been shown, it is possible to obtain the transverse/radial diffusivity and axial diffusivity for each configuration. The average values of transverse/radial and axial diffusivities obtained are: 0.0041 mm^2/h and 0.0113 mm^2/h. Using the diffusion constants

obtained from the regression for each geometry, the analytical and FE predictions were compared to the experimental results, **Fig.12**.

Fig.12 Weight gain curves of: (a) plates, (b) rods and (c) pipes. Theoretical and FE predictions have been obtained using the same material constants obtained from the regression analysis, in **Table 2**.

It is possible to observe that the average diffusion constants obtained with the methodology reported here allow a quite accurate prediction of the diffusion behaviour of different composite structures: plates, rods and pipes. Since all these samples have been obtained from the same laminate and the diffusivity is a material constant, it is important to verify that the weight gain for all geometries can be predicted starting from the same diffusivities. The accuracy of the analytical solutions is further confirmed by the agreement with the FE results.

In **Fig. 13**, the exact solution, for fluid diffusion in an orthotropic pipe Eq. (20), is compared to the approximated solution, Eq. (22). It is possible to notice that the agreement is very good.

Fig.13 Comparison of analytical exact solution (pipes) and approximated solution (plates).

6. Discussions

An experimental methodology, proposed here, enables identifying the orthotropic diffusion constants and saturation level in the most common composite structures used in offshore and marine applications. This is possible adopting short and long rods and pipes. The method proposed here had the advantage of simplicity in manufacturing adequate specimens for each

geometry studied, and the downside that a regression analysis needs to be performed to identify the diffusion constants from the experimental results.

The values of the diffusion constants obtained are quite consistent for all geometries, as shown in **Fig. 11**. The analytical solutions have been also verified by means of FE analysis, yielding good agreement, **Figs. 9,12**.

It can be noticed that transverse/radial diffusivity values from all geometries are very close. Axial diffusivity values are quite close for plates and rods, while pipes yield an overestimation of the axial diffusivity. This effect is attributed to the shape of the samples, having an internal surface that may be hard to reach and dry perfectly. Furthermore, the short pipes need to be handled and dried very carefully, due to the absence of any hoop reinforcement. This difference may limit the effectiveness of drying prior to weighting the samples, hence overestimating the axial diffusivity.

For composite pipes, the approximated analytical solution in Eq. (22), yields very close results to the exact solution, Eq. (20). The comparison of exact and approximated solution can be seen in **Fig. 13**. The possibility of describing fluid diffusion in a pipe using 2-D plate equations has an important application. The influence of matrix cracks in cross ply laminates has been studied extensively for composite laminates [24, 25]. Analytical solutions obtained for these cases can be extended directly for the prediction of fluid diffusion in a pipe having matrix cracks.

Conclusions

The most frequently utilized composite structures in offshore and marine applications are plates, rods (cylinders) and pipes. Due to the exposure to fluid these structures are subjected to fickian diffusion, which influences the mechanical performance of the material. Prediction

of the concentration profiles inside these structures after long exposure times is hard because the knowledge of orthotropic diffusion constants is required for a correct prediction. In this work a novel test method is proposed in order to identify radial/transverse and axial diffusion constants. The diffusion constants are identified comparing the solutions of fluid diffusion equations in cartesian and cylindrical coordinates to the experimental weight gain results. This method is known for composite plates but has never been extended to composite pipes before. In order to verify the validity of this method plates, rods and pipes were obtained from the same laminate, in order to directly compare the diffusion constants obtained from each geometry. The results showed good agreement for all the geometries tested, leading to the conclusion that the method proposed here enables accurate measurement of fluid diffusion constants in composite pipes. The accuracy of the analytical solution for each case (plates, rods and pipes) has been further confirmed by a comparison with FE results.

Finally, an approximated solution has been proposed for the prediction of fluid diffusion behaviour in composite pipes, based on the analogy between a pipe and an infinitely wide plate. The approximated solution was compared to the exact one and yielded a very accurate prediction. This is an interesting fact, because the possibility of predicting the fluid diffusion behaviour of a pipe using a plate solution allows direct use of the equations for the prediction of diffusion in cracked laminates developed for orthotropic plates.

Acknowledgements

This work is part of the DNV GL led Joint Industry Project “Affordable Composites” with nine industrial partners and the Norwegian University of Science and Technology (NTNU). The authors would like to express their thanks for the financial support by The Research Council of Norway (Project 245606/E30 in the Petromaks 2 programme).

The authors would like to thank Prof. Astrid S. de Wijn for interesting discussion on fluid diffusion theory and Mr. Erik Sæter, for the assistance in the samples preparation.

References

1. Springer, G., *Environmental Effects on Composite Materials*. Vol. 1. 1984: Technomic Publishing Company.
2. Springer, G., *Environmental Effects on Composite Materials*. Vol. 2. 1984: CRC Press.
3. Weitsman, Y.J., *Fluid Effects in Polymers and Polymeric Composites*. Mechanical Engineering Series. 2012: Springer US.
4. Whitney, J.M., *Three-Dimensional Moisture Diffusion in Laminated Composites.* AIAA Journal, 1977. **15**(9): p. 1356-1358.
5. Rocha, I.B.C.M., et al., *Combined experimental/numerical investigation of directional moisture diffusion in glass/epoxy composites.* Composites Science and Technology, 2017. **151**: p. 16-24.
6. Gagani, A., Fan Y., Muliana, A.H., Echtermeyer, A.T., *Micromechanical modeling of anisotropic water diffusion in glass fiber epoxy reinforced composites.* Journal of Composite Materials, 2017. **52**(17): p. 2321-2335.
7. Blikstad, M., P.O.W. Sjöblom, and T.R. Johannesson, *Long-Term Moisture Absorption in Graphite/Epoxy Angle-Ply Laminates.* Journal of Composite Materials, 1984. **18**(1): p. 32-46.
8. Beringhier, M., et al., *Identification of the orthotropic diffusion properties of RTM textile composites for aircraft applications.* Composite Structures, 2016. **137**(Supplement C): p. 33-43.
9. Gagani, A., A. Krauklis, and A.T. Echtermeyer, *Anisotropic fluid diffusion in carbon fiber reinforced composite rods: Experimental, analytical and numerical study.* Marine Structures, 2018. **59**: p. 47-59.
10. ASTM, *Standard Test Method for Moisture Absorption Properties and Equilibrium Conditioning of Polymer Matrix Composite Materials*. 2014, ASTM International, West Conshohocken, PA.
11. Chilali, A., et al., *Effect of geometric dimensions and fibre orientation on 3D moisture diffusion in flax fibre reinforced thermoplastic and thermosetting composites.* Composites Part A: Applied Science and Manufacturing, 2017. **95**: p. 75-86.
12. Saidane, E.H., et al., *Assessment of 3D moisture diffusion parameters on flax/epoxy composites.* Composites Part A: Applied Science and Manufacturing, 2016. **80**: p. 53-60.
13. Beringhier, M. and M. Gigliotti, *A novel methodology for the rapid identification of the water diffusion coefficients of composite materials.* Composites Part A: Applied Science and Manufacturing, 2015. **68**: p. 212-218.
14. Gustafson, C.-G. and A. Echtermeyer, *Long-term properties of carbon fibre composite tethers.* International Journal of Fatigue, 2006. **28**(10): p. 1353-1362.
15. Echtermeyer, A.T., *Integrating Durability in Marine Composite Certification*, in *Durability of Composites in a Marine Environment*, P. Davies, Rajapakse Yapa D.S., Editor. 2014, Springer Netherlands: Amsterdam. p. 179-194.
16. Salama, M.M., et al., *The First Offshore Field Installation for a Composite Riser Joint*. Offshore Technology Conference.
17. Grabovac, I. and D. Whittaker, *Application of bonded composites in the repair of ships structures – A 15-year service experience.* Composites Part A: Applied Science and Manufacturing, 2009. **40**(9): p. 1381-1398.
18. McGeorge, D., et al., *Repair of floating offshore units using bonded fibre composite materials.* Composites Part A: Applied Science and Manufacturing, 2009. **40**(9): p. 1364-1380.

19. HEXION, *Technical Data Sheet*, in *EPIKOTE Resin MGS RIMR 135 and EPIKURE Curing Agent MGS RIMH 137* 2006.
20. ASTM, *Standard Test Methods for Constituent Content of Composite Materials*. 2015, ASTM International, West Conshohocken, PA.
21. Crank, J., *The mathematics of diffusion*. 1956, Oxford: Clarendon Press.
22. Barjasteh, E. and S.R. Nutt, *Moisture absorption of unidirectional hybrid composites.* Composites Part A: Applied Science and Manufacturing, 2012. **43**(1): p. 158-164.
23. Roy, S., et al., *Modeling of moisture diffusion in the presence of bi-axial damage in polymer matrix composite laminates.* International Journal of Solids and Structures, 2001. **38**(42–43): p. 7627-7641.
24. Gagani, A.I. and A.T. Echtermeyer, *Fluid diffusion in cracked composite laminates – Analytical, numerical and experimental study.* Composites Science and Technology, 2018. **160**: p. 86-96.
25. Roy, S. and T. Bandorawalla, *Modeling of Diffusion in a Micro-Cracked Composite Laminate Using Approximate Solutions.* Journal of Composite Materials, 1999. **33**(10): p. 872-905.

Appendix

In this appendix are reported the results of a parametric study comparing the exact solution of the mass increase with time, Eq. (20), and the approximated solution, (Eq. 22), for fluid diffusion in an orthotropic pipe.

The material constants used for this parametric analysis are the same ones measured in this study:

- $M_{eq} = 0.775\%$
- $D_R = 0.0041\ mm^2/h$
- $D_Z = 0.0113\ mm^2/h$

The dimensions chosen are also based on the geometry analysed in this work: the external radius was 12 mm, the length of the pipe was 20 mm. The values of internal radius analysed were 4 mm, 6 mm, 8 mm and 10 mm, equivalent to a wall thickness to external radius ratio t/r_e: 0.667, 0.5, 0.33 and 0.167.

For most engineering applications, a t/r_e ratio smaller that 0.33 is adopted, which results in a deviation between the slope predicted by the exact solution and by the analytical solution below 1 %, **Fig. A.1**. Since both theoretical models employ the same diffusivity constants,

the slopes of the mass increase curves are compared. Examples of mass increase curves are shown in **Figs. 9, 12, 13**.

For a very thick-walled pipe, having a wall thickness equal to half of the external radius ($t/r_e = 0.5$), the deviation is 6.1 %, which is still a quite reasonable estimate. Finally, for an extremely thick-walled pipe, having a wall thickness equal to 2/3 of the external radius ($t/r_e = 0.667$), the deviation is 15.7 %, which suggests that the limit of validity of the approximated solution has been reached.

Fig.A.1 Parametric comparison of analytical exact solution (pipes) and approximated solution (plates)

It can be concluded that for the set of material properties studied here, which is representative of a fiber reinforced composite, the approximated solution for the analysis of fluid diffusion in pipes is quite accurate in a wide range of pipe wall thickness values. In particular the deviation between the weight gain slope predicted is below 1 % for a wall thickness up to 1/3 of the external radius of the pipe.

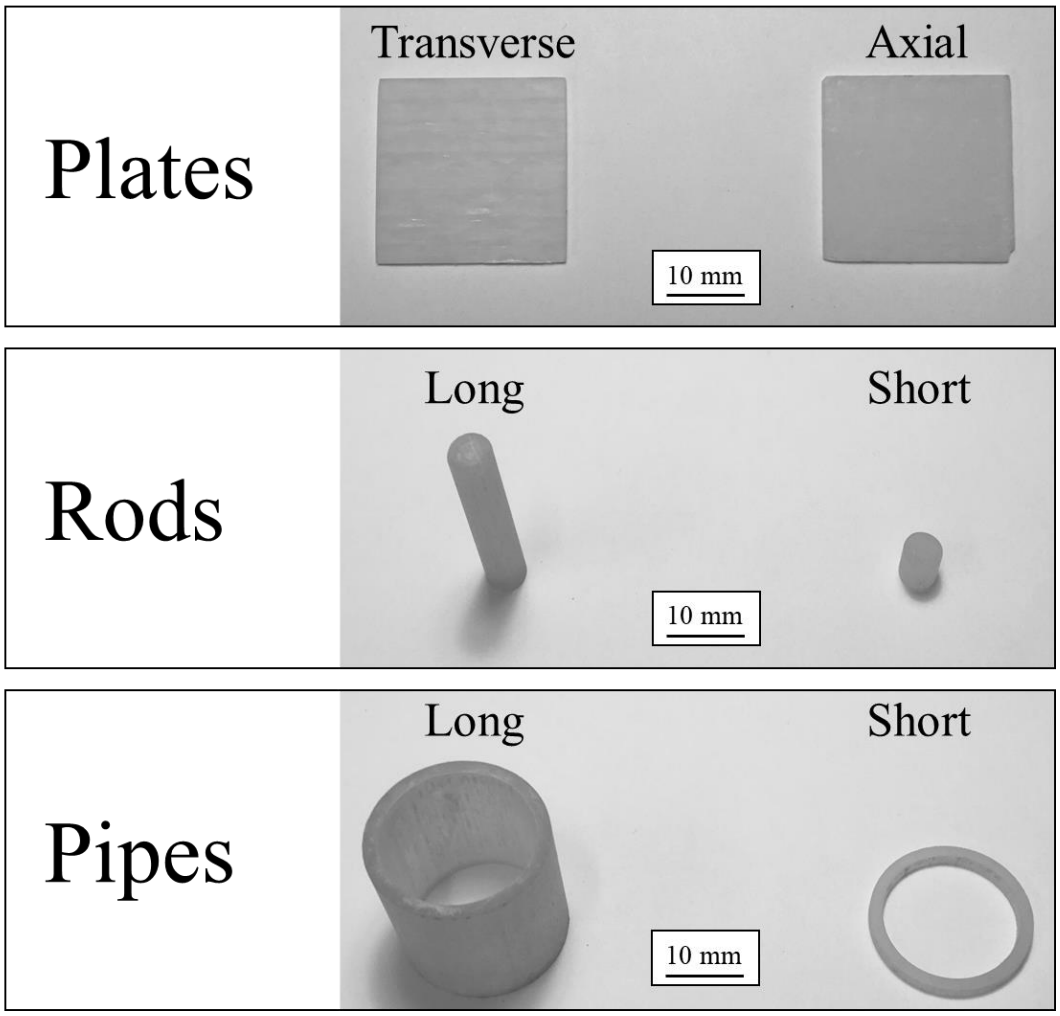

Fig. 1. Sample configurations tested

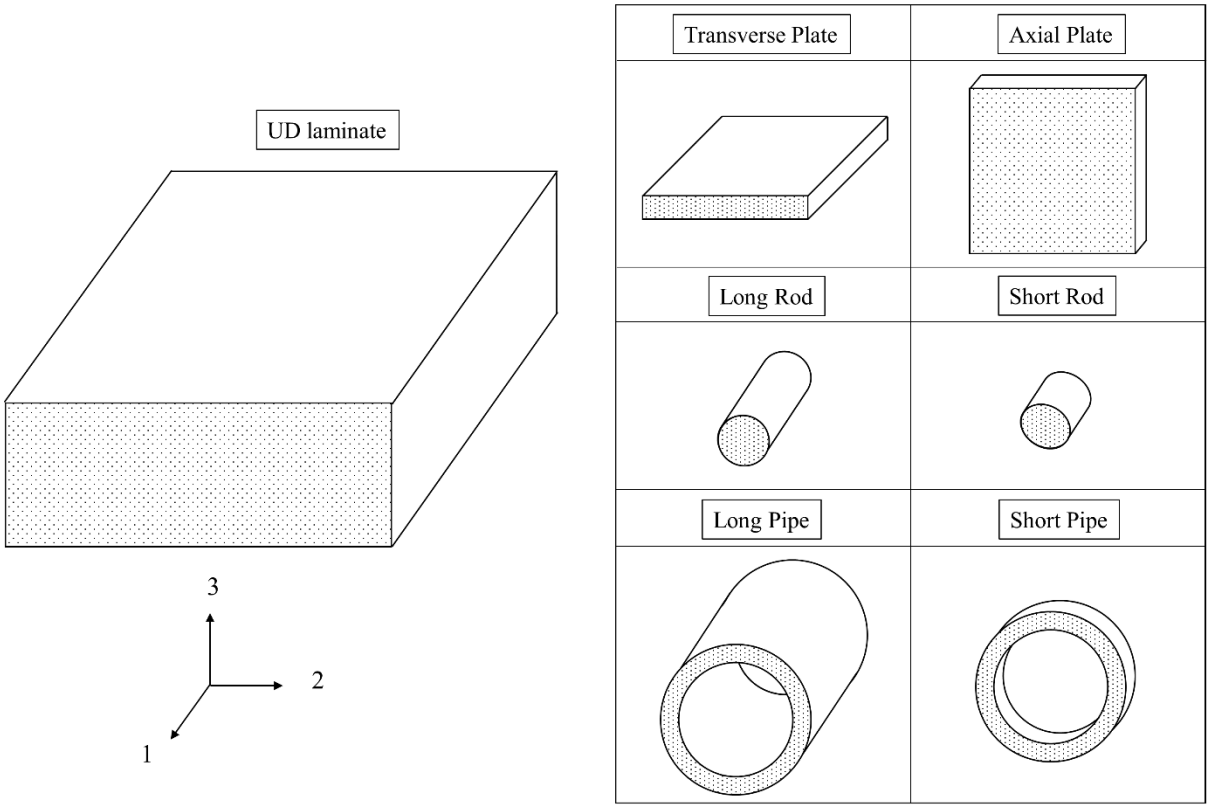

Fig. 2. Sample configurations for plates, rods and pipes. It can be noticed that for rods and pipes the axial direction coincides with the laminate fiber direction

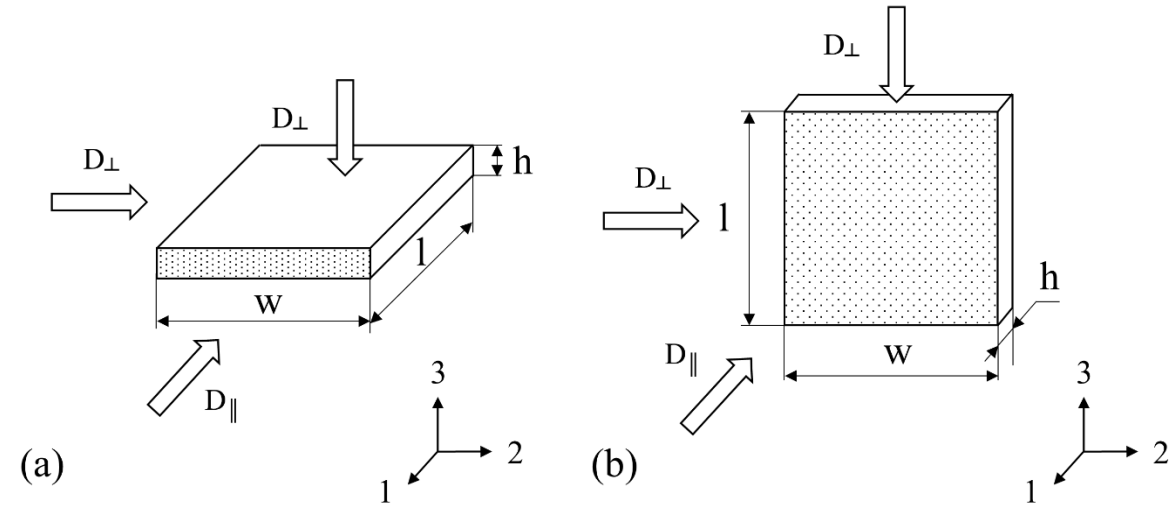

Fig. 3. (a) Transverse plate geometry, **(b)** Axial plate geometry

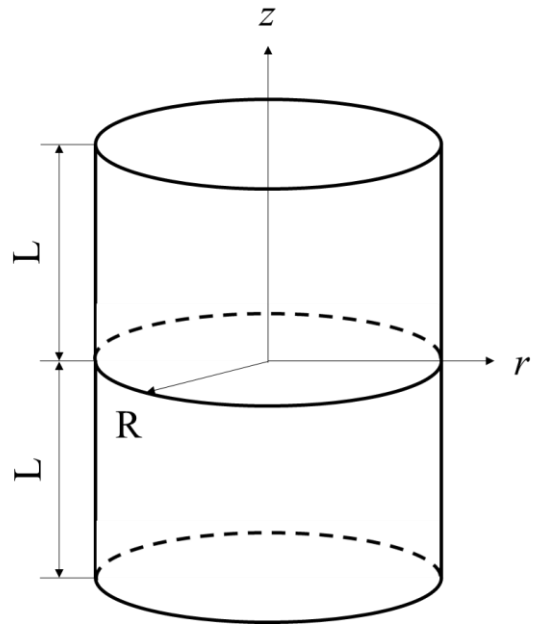

Fig. 4. Coordinate system and dimensions for a composite rod

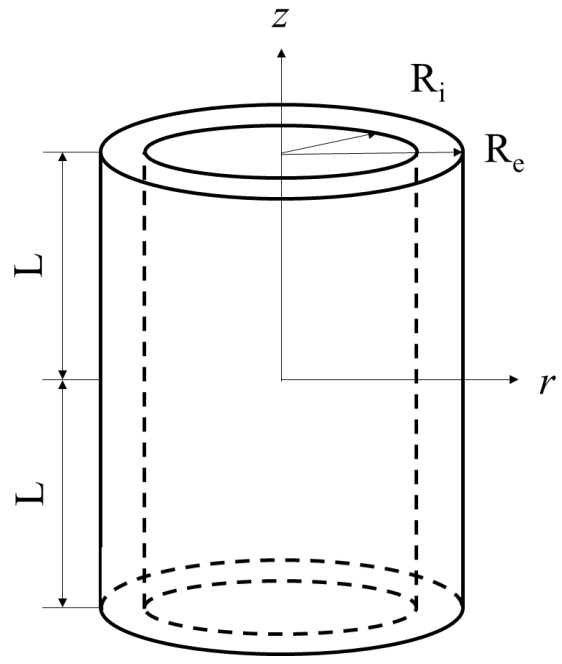

Fig. 5. Coordinate system and dimensions for a composite pipe

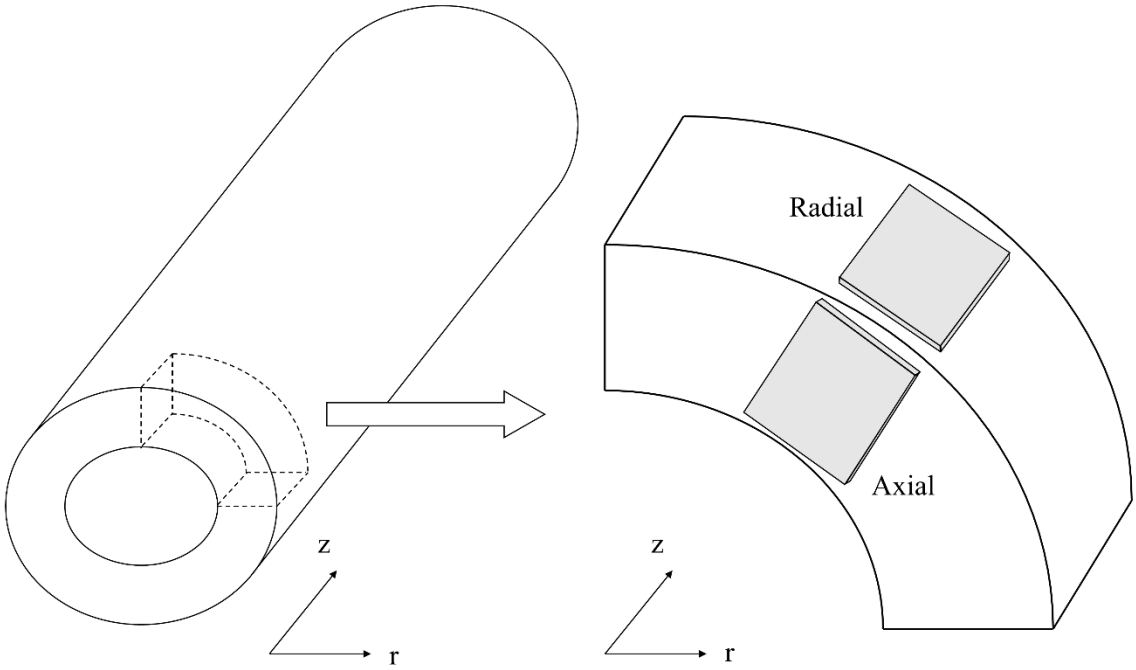

Fig. 6. Schematic drawing on obtaining axial and radial diffusion plates from a thick-walled pipe

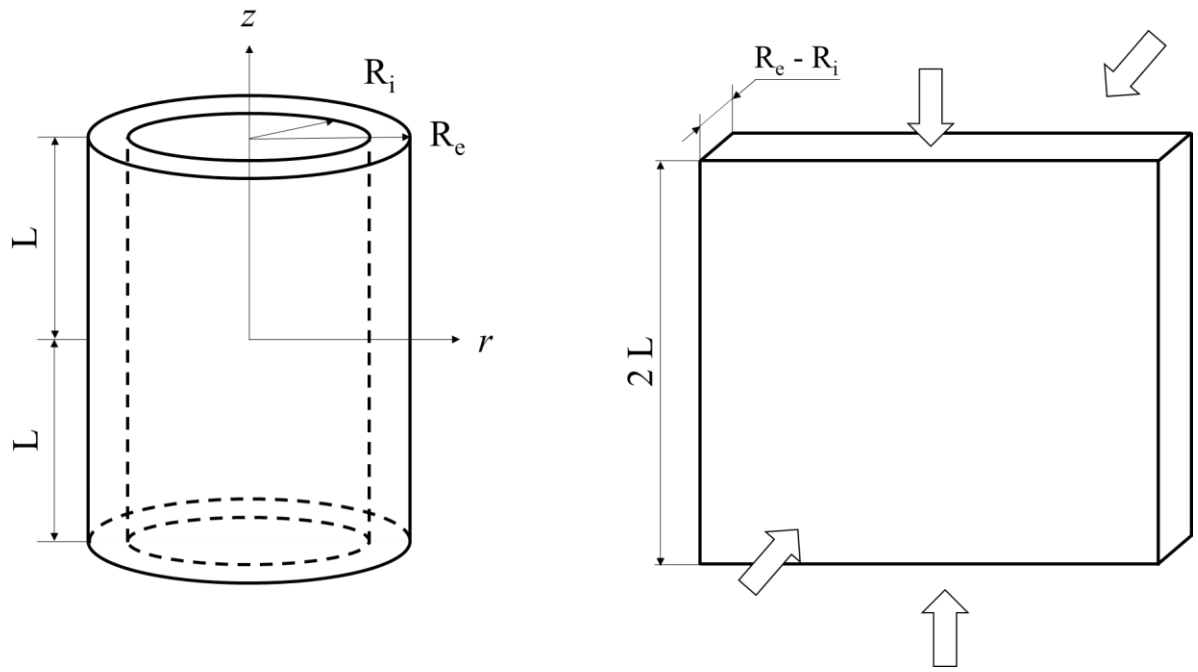

Fig. 7. Approximation of thin-walled pipe to equivalent infinitely wide plate

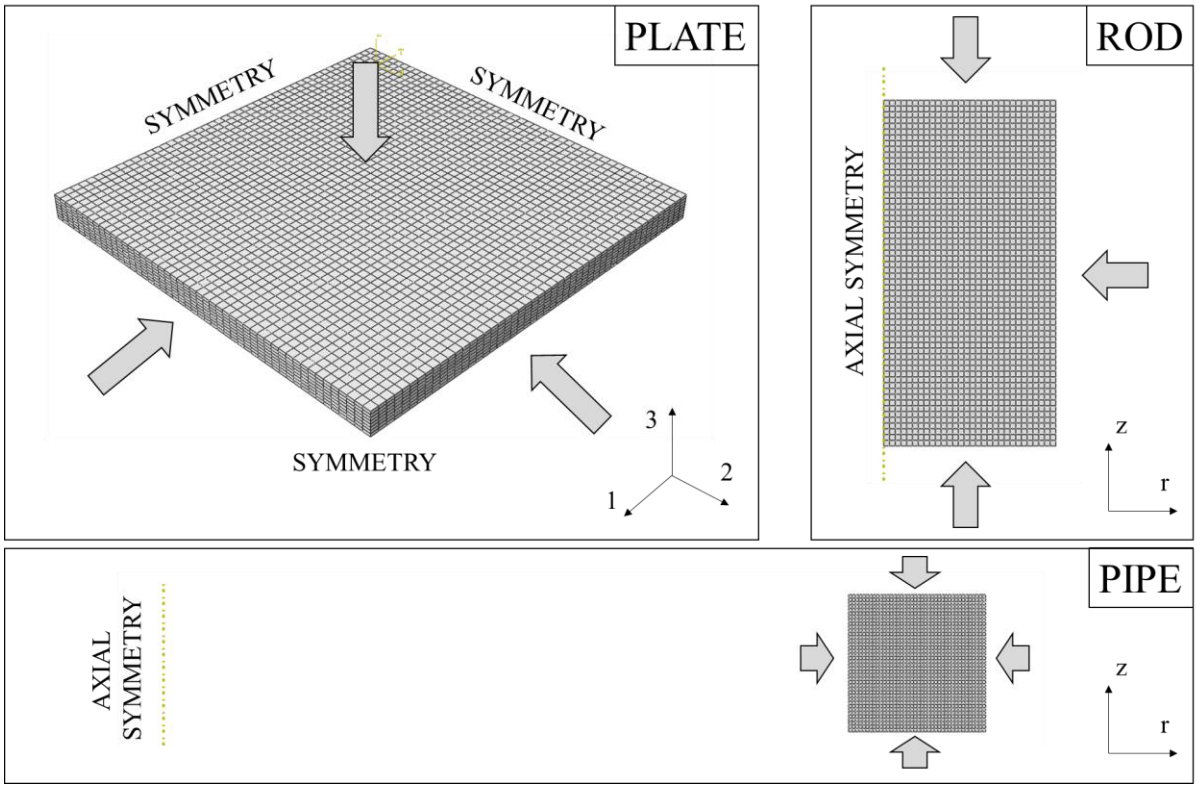

Fig. 8. FE models used for the plate, rod and pipe. The surfaces exposed to fluid diffusion are indicated by the arrows

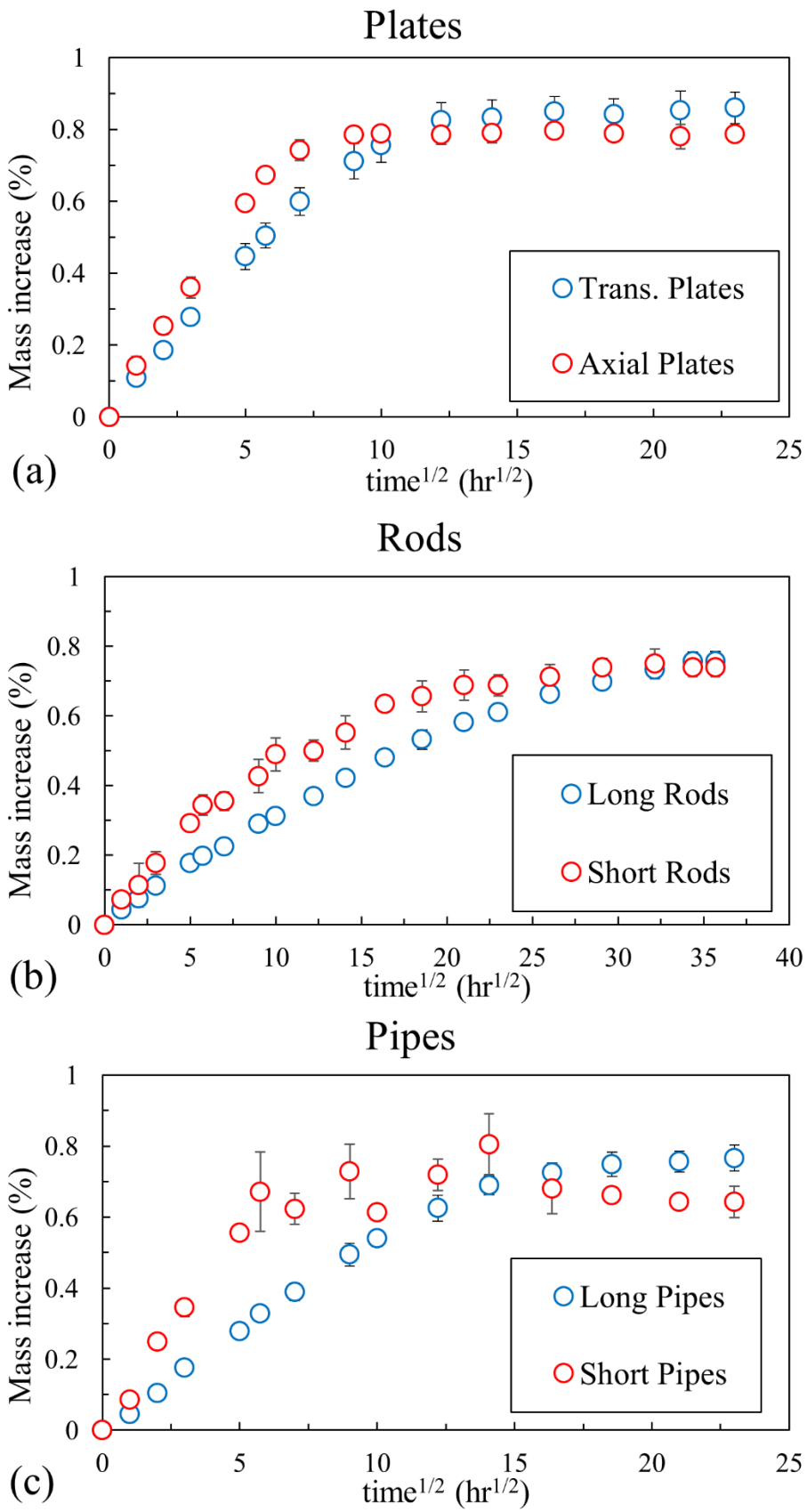

Fig. 9. Experimental weight gain curves of: (a) plates, (b) rods and (c) pipes.

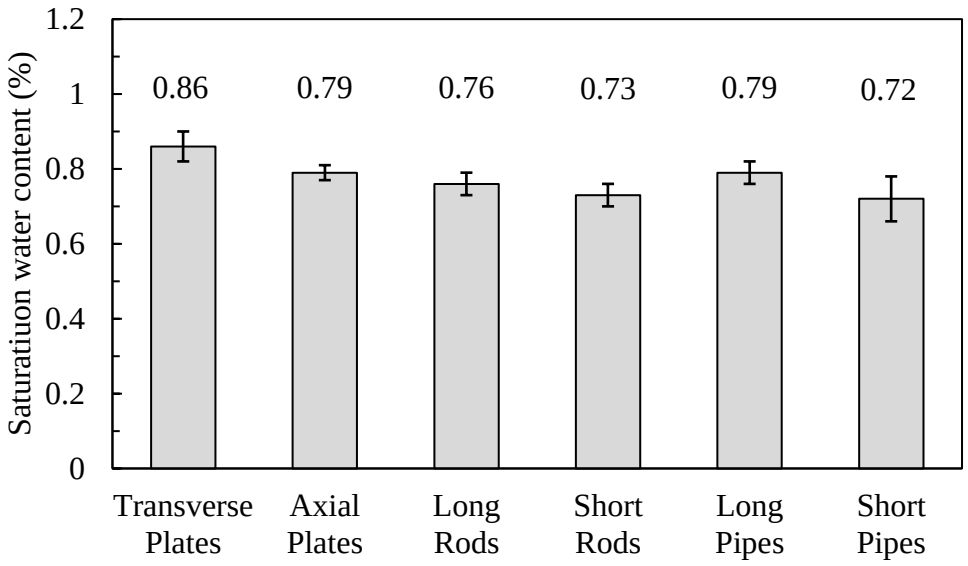

Fig. 10. Moisture saturation content for each configuration

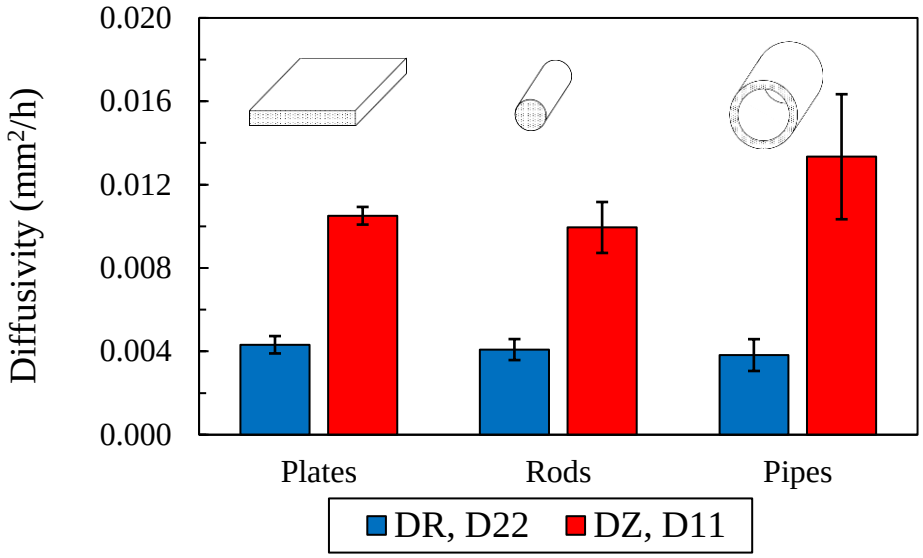

Fig. 11. Diffusivities for each geometry (plates, rods, pipes)

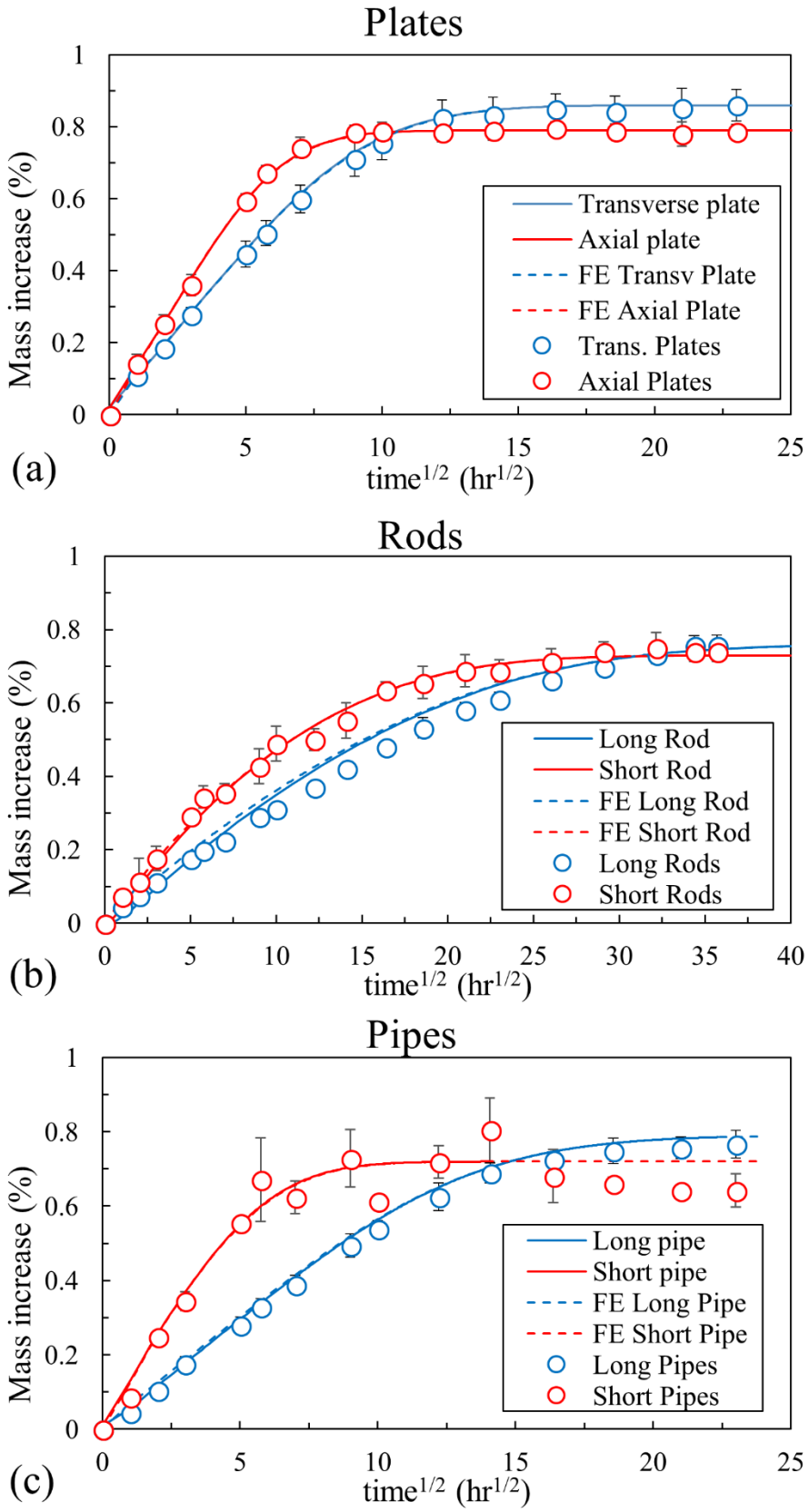

Fig.12 Weight gain curves of: (a) plates, (b) rods and (c) pipes. Theoretical and FE predictions have been obtained using the same material constants obtained from the regression analysis, in **Table 2**.

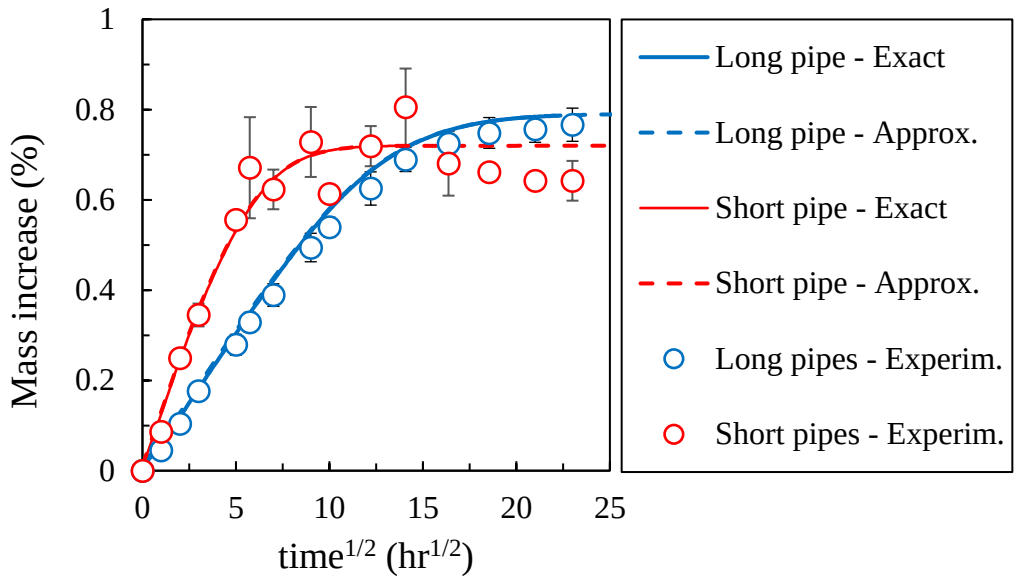

Fig.13. Comparison of analytical exact solution (pipes) and approximated solution (plates).

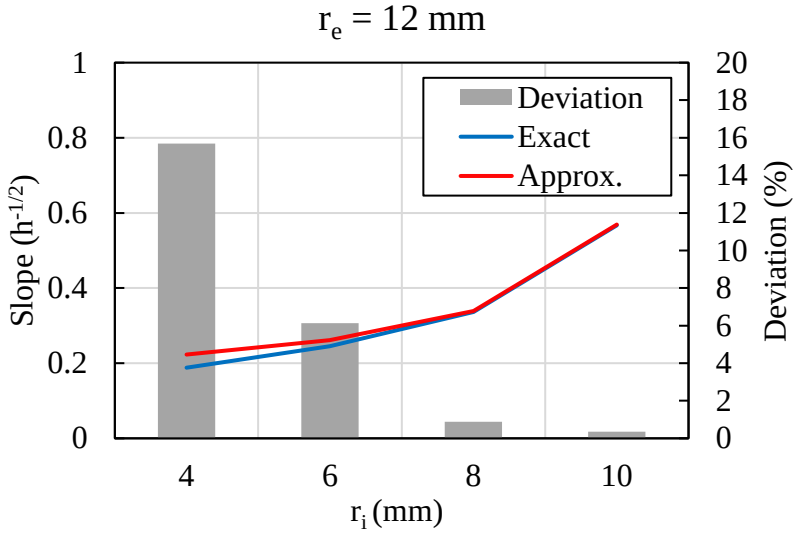

Fig.A.1. Parametric comparison of analytical exact solution (pipes) and approximated solution (plates).